

Ultrasound Tomography for Spatially Resolved Melt Temperature Measurements in Injection Moulding Processes

Hopmann C and Wipperfurth J *

Institute of Plastics Processing (IKV), RWTH Aachen University, Seffenter Weg 201, 52074 Aachen, NRW, Germany

Abstract

In injection moulding processes, the measurement of the temperature distribution is very important for the validation of models used for simulative part design due to the high influence on shrinkage and warpage of the moulded part, but is also very challenging to measure. During the injection moulding process high mould pressures occur and the cavity is not easily accessible. Therefore, contact sensors cannot be used since they induce shear stress into the melt, which changes the flow behaviour of the melt and thus the temperature field. In this work, we present a method for the contactless determination of the temperature distribution of a moulded part during injection moulding using ultrasound tomography. With time-of-flight ultrasound measurements from different directions it is possible to reconstruct the distribution of ultrasound velocity in the cross-section of a moulded part. With this distribution, the temperature field can be calculated using additional material characteristic properties. Based on this concept, an injection mould was designed, that allows performing ultrasound tomography with 20 ultrasound transducers radially arranged around a cylindrical shaped cavity. This allows the temperature determination under real process conditions with a spatial resolution of 3.5 mm². A highly parallelised measurement device allows recording of several complete datasets before no more signals can be detected due to shrinkage of the moulded part. During several injections moulding-cycles all sensor positions were able to detect noticeable signals. Due to internal signal processing of the measurement device, it is not yet possible to calculate arrival times of the ultrasound signal but amplitude-scans show the general feasibility of ultrasound tomography during injection moulding..

Keywords: Temperature; Injection moulding; Tomography; Ultrasound

Introduction

The quality of moulded plastics parts, such as shrinkage, warpage; mechanical and thermal properties are highly influenced by the injection moulding process [1]. In the last years, the increasing requirements for quality and accuracy of moulded parts lead to a significant need of simulation and are routine tools for the engineer in the meanwhile to predict accurately the properties of the final parts [2,3]. A lot of commercial software is available on the market, such as Moldflow, Sigmasoft, Moldex3D and Cadmould. Each of the software uses different models and approaches to describe parts of the injection moulding process and their effect on the moulded part. In the injection moulding process the main parameters are injection time, pressure, mould temperature and melt temperature [2]. While injection time, pressure and mould temperature can be described accurately via theoretical models and validated under injection moulding conditions, the melt temperature is still a challenging parameter. The temperature history of a moulded part is complex to describe theoretically due to high cooling rates, complex heat transfer mechanisms to the mould and the forming microstructure especially with respect to semi-crystalline thermoplastics. However, the knowledge of the temperature field of a polymer in the cavity during the injection moulding process is required to perform precise simulations for the prediction of shrinkage and warpage of the moulded part. Today's measurement techniques, such as thermocouples, are still based on the direct contact between sensor and melt, which influences the melt flow and induces shear stresses. Furthermore, only punctual information can be obtained with high response times, which prevent precise temperature measurements and thus a detailed process understanding. Therefore, contact measurement techniques are not suitable for the determination of the real temperature. Other sensor techniques, such as IR-Sensors, do not require direct contact but special sapphire windows to measure the punctual temperature at or near the surface [4]. This is adverse, e.g.

for the validation of newly developed models used in part design, since the temperature is measured under a different contact behaviour at the interface of the melt and the cavity wall. In this context, an increasing importance for non-invasive measurement techniques is caused by these disadvantages. Several different research approaches were carried out in the last years, such as pyrometry [5], fluorescence spectroscopy [6] or ultrasound [7-9]. Recent approaches base on the use of tomographic methods to measure the local temperature distribution. There are two current approaches: the ultrasound tomography [8,9] and the electrical capacitance tomography (ECT) [10]. Both methods have in common that signals can be introduced into the melt from different directions. Due to interactions of the radiation with the melt, various sensors, around the measurement region, can measure a response. Using this, distribution ultrasound velocities can be calculated and correlated with the local temperature. In the case of ultrasound tomography first the distribution of ultrasound velocities is calculated based on the time of flight measurements and then the temperature field is calculated with the help of further material properties such as the bulk modulus and the shear modulus. The ultrasound tomography used in this work is based on the procedure of Praher et al. [8] who suggests using ultrasound signals to measure the temperature field in the screw antechamber of an injection-moulding machine and assumed a radial symmetric temperature distribution to realise a fast temperature

*Corresponding author: Jens Wipperfurth, Institute of Plastics Processing (IKV), RWTH Aachen University, Seffenter Weg 201, 52074 Aachen, NRW, Germany, Tel: +49 241 80 28364; E-mail: jens.wipperfuerth@ikv.rwth-aachen.de

Received March 08, 2017; Accepted May 22, 2017; Published May 26, 2017

Citation: Hopmann C, Wipperfurth J (2017) Ultrasound Tomography for Spatially Resolved Melt Temperature Measurements in Injection Moulding Processes. J Appl Mech Eng 6: 264. doi: [10.4172/2168-9873.1000264](https://doi.org/10.4172/2168-9873.1000264)

Copyright: © 2017 Hopmann C, et al. This is an open-access article distributed under the terms of the Creative Commons Attribution License, which permits unrestricted use, distribution, and reproduction in any medium, provided the original author and source are credited.

measurement with only five ultrasound transducers. In this work, we present an extended approach to measure the temperature distribution of a moulded part during injection moulding and solidification that will focus on the spatial resolution. The advantage of this measurement technique is the stability against the high cooling rates and complex heat transfer mechanisms prevailing during the injection moulding process, since the acquired data include this information. In future, the knowledge of the temperature distribution and its evolution during the process will considerably improve the simulative part design.

Principle of Ultrasound Tomography

In ultrasound-time-of-flight (TOF) tomography, an ultrasound transducer emits an ultrasound wave that propagates through the melt. A set of receiving transducers radially arranged around the region of interest measures the arrival time of the emitted wave that is used for the reconstruction of the distribution of ultrasound velocity. Typically, tomographic methods require consecutive measurements from different directions. This requires a rotation of either the sample or the sensor-detector-arrangement. In our approach of ultrasound tomography, a rotation is not required since the transducers are able to both emit and detect ultrasound signals.

Between an ultrasound emitter and an ultrasound receiver one can assume that an emitted ultrasound wave propagates along the path g between the emitter and the receiver. The ultrasound wave can be detected at the opposite receiver after an arrival time $t_{tot} = t_E - t_D$, which is the difference of the start time of the propagation t_0 and the detection time t_E . The time required for the ultrasound wave to traverse the melt depends on the ultrasound velocity c that is a temperature and pressure dependent material property. However, along the path g many different transit times t_{ik} that arise from different ultrasound velocities due to temperature inhomogeneity, determine the arrival time t_{tot} . That means by discretising the measurement region into $j \times l$ arbitrary subareas s the arrival time can be expressed as the amount of the propagation times t_{ik} in an individual subarea s_{ik} (equation (1)). Further, each transit time t_{ik} can be expressed in terms of the ultrasound velocity c_{ik} . For this purpose, the length of each path \bar{g} in a subarea s_{ik} has to be known. This can be done by introducing a factor b_{ik} that scales the length of \bar{g} in s_{ik} .

$$t_{tot} = \sum_{s_{i=1, k=1}}^{s_{jl}} t_{ik} = \sum_{k=1}^l \sum_{i=1}^j \frac{b_{ik}}{c_{ik}}(T) \quad (1)$$

From equation (1), it is clear that the transit times in every subarea s_{ik} are needed to solve the equation for c_{ik} . In practice, this is realised by measuring the transit times from different directions.

Furthermore, equation (1) is valid for n emitter/receiver-paths \bar{g}_n . Considering this, a system of linear equations can be set up as shown in equation (2) where in,

$$a_{n, ik} = b_{ik}(\bar{g}_n) \begin{pmatrix} a_{11} & \dots & a_{1, jl} \\ \vdots & \ddots & \vdots \\ a_{n1} & \dots & a_{n, jl} \end{pmatrix} \begin{pmatrix} 1/c_1 \\ \vdots \\ 1/c_{jl} \end{pmatrix} \quad (2)$$

The Matrix in equation (2) includes the information of the individual path lengths $b_{ik}(\bar{g}_n)$. This matrix is multiplied with the corresponding reciprocal ultrasound velocity c_{ik} in the element s_{ik} and the result is a vector, containing the measured transit times for every path \bar{g} . Equation (2) can be expressed in a general form:

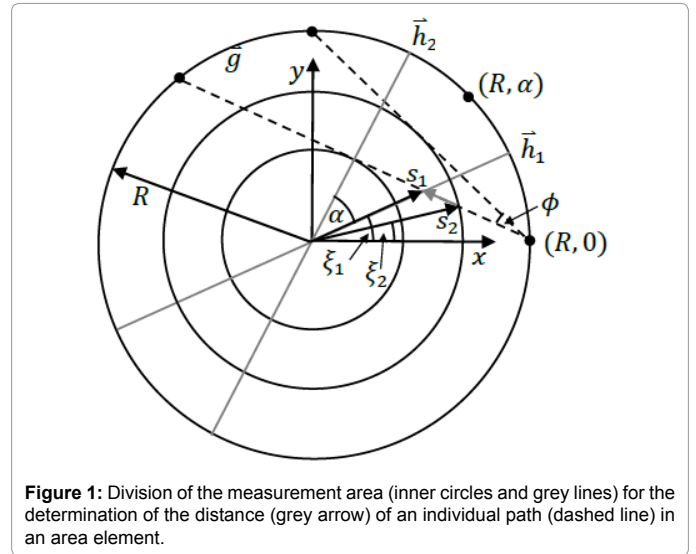


Figure 1: Division of the measurement area (inner circles and grey lines) for the determination of the distance (grey arrow) of an individual path (dashed line) in an area element.

$$A\bar{c} = \bar{t}_{tot} \quad (3)$$

The matrix A is often called design matrix or system matrix in the literature [11]. This should clarify that A is constructed using information about the structure of the observed measurement region. However, to solve equation (3) for c_{ik} first the system matrix A has to be determined and subsequently an inversion of equation (3) is required.

To construct A , the measurement (Figure 1) region has to be divided into subareas, so that more than one individual path crosses each subarea. This ensures that for each area, sufficient information is available to reconstruct the ultrasound velocity in this element. For this purpose, a Cartesian coordinate system is defined at first, which origin coincides with the centre of the measurement region (Figure 1). In a first step, the measurement region is divided in different circular subareas. The circuits are designed so that each circuit is spanned tangentially to a path g_n . The radii r_n of each circular subarea can be described by equation (4):

$$r_i = R \cos\left(\frac{\alpha_n}{2}\right) \quad (4)$$

In equation (4) R is the radius of the measuring region and α_n is the angle between two sensors and the origin of the coordinate system and results for a given sensor n from the total number of sensors

$$N : \alpha_n = \frac{2\pi}{N}(n-1), n = \{1, \dots, N\} \quad (5)$$

The division of the measuring region however, can be further divided (Figure 1). To this end, additional lines h are defined (Figure 1, grey lines) which are passing through the origin of the coordinate system and through the centre of the distance between two sensors. This can be expressed as a function of α , where v is the scaling factor for the direction vector:

$$\bar{h} : v \begin{pmatrix} \cos\left(\alpha + \frac{\Delta\alpha}{2}\right) \\ \sin\left(\alpha + \frac{\Delta\alpha}{2}\right) \end{pmatrix} \quad (6)$$

To set up the system matrix A successfully, in a next step, the path length of the ultrasound wave has to be calculated in an area segment. A line g that represents the path of the ultrasound wave from an emitter to any receiver, can be described by equation (7):

$$\bar{g} : R \begin{pmatrix} \cos(\varphi) \\ \sin(\varphi) \end{pmatrix} + \mu \begin{pmatrix} \cos(\pi - \alpha) \\ \sin(\pi - \alpha) \end{pmatrix} \quad (7)$$

In equation (7) μ is a scaling factor and ϕ is the angle between two paths and can be calculated using equation (8):

$$\varphi = \frac{\pi}{2} \left(1 - \frac{2n}{N} \right) \quad (8)$$

From the intersection of \bar{g} and \bar{h} and from the intersections of \bar{g} and the circuits, which are described by r_p , the length of the path can be calculated in a subarea by (Figure 1, grey arrow):

$$d = \left| \bar{g}(s_1) - \bar{g}(s_2) \right| = r_i^2 + r_{i+1}^2 - 2 \cos(\xi_1 - \xi_2) \quad (9)$$

To calculate the matrix A, the relations described above have been implemented in a routine in the software Matlab 2016a (The MathWorks Inc., MA; USA). For an efficient calculation, it is sufficient to describe the radiation extinguished from a specific sensor. Furthermore, the routine has to calculate the paths only for one semi-cycle, the other semi-cycle can be achieved by mirroring (Figure 2).

In the routine, the resulting distances for one ray path are stored in a table of the form shown in Figure 2.

For each ray path at one sensor position such a table is calculated. By moving each row to the row beneath, the next sensor position can be fully described. From this, the distances of all ray paths for each area element can be determined for a specific measurement region (Figure 3, left) that has a defined radius and a specified number of ultrasound transducers (Figure 3, white circles). To create the system matrix the rows of one table are concatenated into one row. Subsequently, the rows are strung together and form the system matrix (Figure 3, right). The system matrix thus has N(N-1) rows and the number of columns

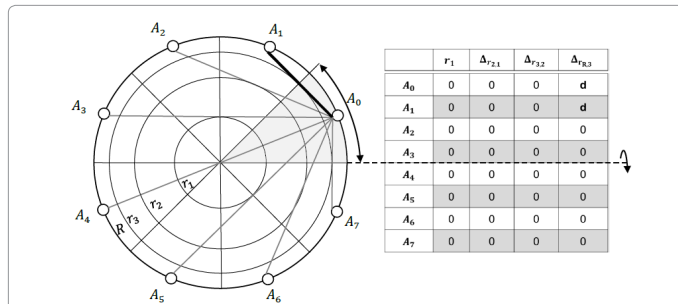


Figure 2: Storage of the distances of one path emanated from a specific sensor. The table shows the distances of the illustrated path (bold black line) for every area element in the measurement region. Since the path only traverses two area elements most of the values are zero.

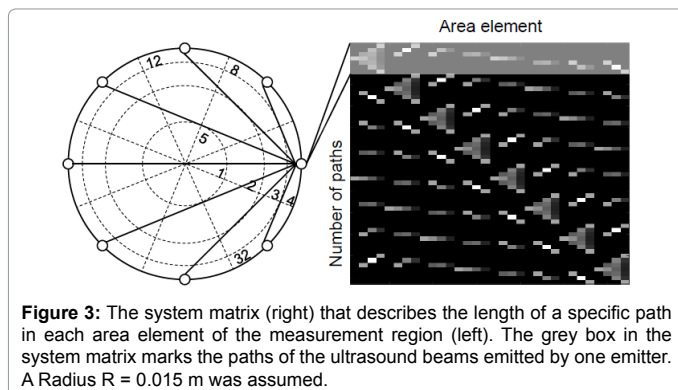


Figure 3: The system matrix (right) that describes the length of a specific path in each area element of the measurement region (left). The grey box in the system matrix marks the paths of the ultrasound beams emitted by one emitter. A Radius R = 0.015 m was assumed.

describes the number of area elements 1 - 32. It can be followed that the system matrix includes the information of the distance for each ray in every area element. The entries represented in black in Figure 3 are zero-entries, which mean that the specific ray does not pass that area element. However, values greater than zero represent a distance of a beam through that area element and the higher the grey value the longer the distance. Since A has many zero entries, it is suitable to store the matrix as a sparse matrix, which is only for the efficiency of the routine.

To calculate the individual ultrasound velocities from the measured transit times, the system of equations in equation (3) has to be inverted. Due to A, this system of equations is overdetermined so that no direct solution can be obtained. Therefore, iterative reconstruction techniques like ART (Algebraic Reconstruction Technique), SIRT (Simultaneous Iterative Reconstruction Technique) or SART (Simultaneous Algebraic Reconstruction Technique) have to be applied. The procedure of each iterative reconstruction technique is explained and discussed in the literature in detail [12]. In this work, the SART algorithm is used [13] that provide high accuracies [12]. The algorithm is part of the Matlab open source package AIRtools of the Technical University of Denmark [13]. The input parameters for the algorithm are the system matrix A, a vector t that contains the measured arrival times and the number of iterations k that should be performed.

Spatial resolution

The dimension of an area element defines the spatial resolution. This means, that each segment of a cycle has another spatial resolution. Mathematically the dimension of an area element is defined by equation (10).

$$A(r, \alpha) = \int_{r_{n-1}}^{r_n \leq R} \int_0^{2\pi/N} r d\alpha dr \quad (10)$$

Since the ultrasound transducers are equidistantly arranged around the radial measurement region it follows $d\alpha = \Delta\alpha = const$ and equation (10) becomes:

$$A_\alpha(r) = \Delta\alpha \int_{r_{n-1}}^{r_n \leq R} r dr \quad (11)$$

From equation (10) and (11) it is clear, that only the total amount of ultrasound transducers has an influence on the spatial resolution. This causes a huge difference to conventional tomography, like x-ray tomography, where the spatial resolution is a function of both the rotation step and the total amount of detector elements. In our approach of ultrasound tomography, the rotation step is only a function of the number of detector elements. Therefore, with a static sensor arrangement one resolution-influencing parameter is lost. However, this is only a minor restriction, since rotations would be hardly realisable under injection moulding conditions and would cause high measurement times. The spatial resolution of an area element in an assumed measurement region with a radius of 0.015 m and eight sensors is about 20 mm². Assuming 20 transducers in a measurement region with the same radius, the spatial resolution increases to 3.5 mm².

Dependence of temperature and ultrasound velocity

The inversion of equation (3) is directly related to the desired goal of a non-invasive determination of the temperature distribution in a polymer melt channel. However, up to this point the temperature is still an unknown quantity. To determine the temperature distribution,

it is necessary to convert each reconstructed ultrasound velocity at a specific location into a local temperature. The coherence shown in equation (12) of the ultrasound velocity c and the temperature T can be attached on the density ρ of the polymer [14].

$$c(x, y) = \left[\frac{1}{\rho(x, y)} \left(K + \frac{4G}{3} \right) \right]^{1/2} \quad (12)$$

In equation (12), K is the adiabatic bulk modulus and G is the shear modulus of the polymer melt. From equation (12), it is clear that for the determination of the temperature distribution, additional material-specific characteristic data has to be known. The density and the compression modulus can be described via Tait approach [5]. In this work, the Tait approach for a semi-crystalline polypropylene (PP505P, Saudi Basic Industries Corporation, Riyadh, Kingdom of Saudi Arabia) is used (Figure 4).

From the pVT -relationship the bulk modulus can be calculated using the adiabatic compressibility κ (equation (13)) [8]:

$$K^{-1} = \kappa = -\frac{1}{v} \left[\left(\frac{\partial v}{\partial p} \right)_T + \frac{T}{c_p} \left(\frac{\partial v}{\partial T} \right)_p \right] \quad (13)$$

The shear modulus relates to the bulk modulus and Young's modulus E via the fundamental equation (14).

$$G = \frac{3KE}{9K - E} \quad (14)$$

In the melt state the shear modulus can typically be neglected [8], but for the solid-state Young's modulus has to be described in dependence of the temperature. For this, tensile tests (Z100, Zwick Roell AG, Ulm, Germany) in a climatic chamber from 30°C to 80°C with 10°C per step were performed with polypropylene (PP). To provide a sample with homogenous temperature, the tensile bars were

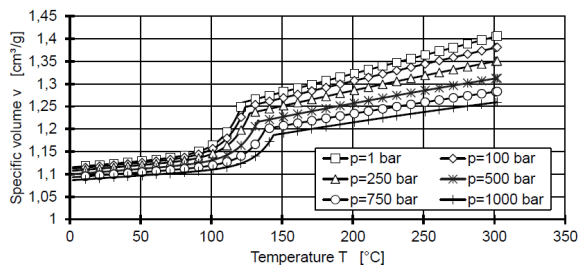


Figure 4: Calculation of the pVT -relation of a polypropylene via Tait-model.

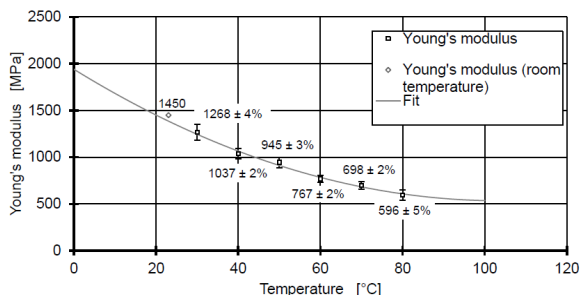


Figure 5: Experimental determination of Young's modulus in dependence of the temperature. The data points represent the mean values of five tensile tests at each temperature. The error bars represent the doubled standard deviation for a better illustration. For this reason, the single relative standard deviation for each data point is specified numerically.

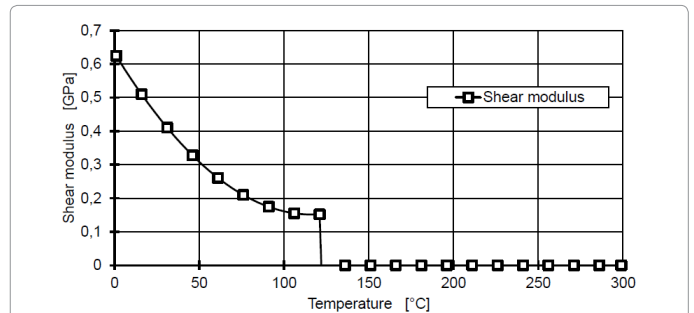


Figure 6: Determination of the temperature dependent shear modulus.

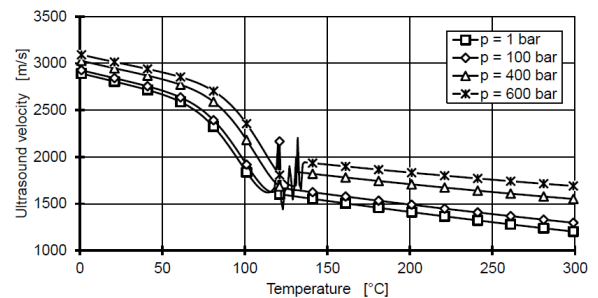


Figure 7: Calculated ultrasound velocity in dependence of the temperature.

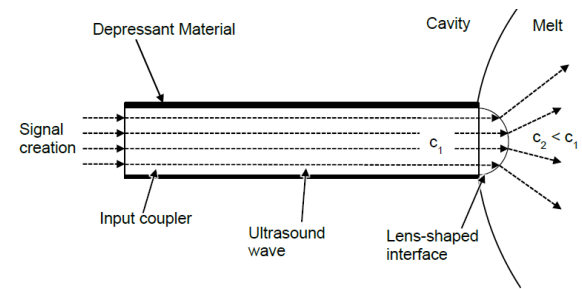


Figure 8: Concept of the buffer rods and the behaviour of ultrasound at curved boundary surfaces.

stored for 16 h in the climatic chamber for each temperature. We use the optical system LIMESS Messtechnik und Software GmbH, Krefeld/Germany, to measure the strain of five tensile bars at each temperature (Figure 5). In order to compare the experimentally determined data, Young's modulus of Sabic PP505P is presented at room temperature from literature [15].

With experimentally determined Young's modulus and the assumption that the shear modulus is neglectable in the melt the shear modulus can be determined (Figure 6).

From the equations (12) - (14) the ultrasound velocity in dependence of the temperature can be calculated (Figure 7). The discontinuity near the melt temperature arises from the pVT behavior of semi crystalline thermoplastics, since the transition from solid to melt state cannot be described by linear relations.

The ultrasound velocity depends on the pressure and temperature conditions prevailing in the melt. In this context, the pressure is always assumed constant in the measurement region so that only local variations in temperature result in local changes in the ultrasound velocity. This results from the intended application to integrate the ultrasound-tomographic measurement concept into an injection

mould. Here, no pressure gradient within a cross section of the flow channel is assumed, which prevails perpendicular to the flow direction [16]. Of course, the pressure in the measurement area has to be known and thus has to be monitored during the injection moulding process.

Properties of ultrasound transducers and constructional challenges

At this point, the theory of ultrasound tomography is fully described. However, for practical realisation analytics on the real behaviour of ultrasound transducers has to be done. In the assumption made above, a fan shaped propagation of the ultrasound wave was assumed. Depending on the sensor geometry the real propagation profile of an emitted ultrasound wave can be divided into two parts: The near field or Fresnel-zone and the far-field or Fraunhofer-zone [17]. The propagation behaviour in the Fresnel-zone is simple straight, while in the Fraunhofer-zone the ultrasound wave begins slightly to diverge. This behaviour is adverse for the usage in tomography. However, this problem can be solved, using lens-shaped interfaces. If an ultrasonic beam applies to an interface of two media, the beam is reflected, scattered and refracted, but if the surface is curved, the interface behaves similar to a lens in geometrical optics.

Mathematically, a modified lens equation describes the behaviour of ultrasound waves at a curved interface [18]:

$$\frac{1}{b} + \frac{c_1 / c_2}{g} = \frac{1}{f} \quad (15)$$

In equation (15), b is the image distance, c_1 and c_2 are the ultrasound velocity of two media, the distance of the transmitter to the apex of the curvature and f describes the focal point.

The ultrasound velocities of the two media and the direction of the curvature play a determining role. Depending on the ratio of the two ultrasound velocities the ultrasound wave either is focused or

diverges in terms of a particular direction of the curved interface. This behaviour changes if the direction of the curvature is changed. For the use of ultrasound tomography in the injection moulding process, one can expect that the ultrasound velocity of the melt is much smaller than the ultrasound velocity of the mould, which is made of steel. From this follows, that the curvature must have a convex form (Figure 8). For this reason, additional buffer rods have to be used that direct the ultrasound wave through the mould in the melt (Figure 8). To avoid any circulations of the ultrasound wave within the mould these input couplers must be coated with a depressant material. One end of the buffer rod, which directs to the melt, has a convex form; the other end is a planar area, which is used to mount the ultrasound transducer.

The theory of scattering the ultrasound wave at curved interfaces confirms the results of Praher et al. who tried different geometries to scatter an ultrasound wave and identified the lens-shaped geometry as the best working one [8]. The usage of input couplers is beneficial since they shield the temperature sensitive ultrasound transducers.

Results and Discussion

Virtual test problems

For later reconstructions of the temperature distribution, it is important to evaluate the accuracy of the algorithm first. Less importance is attributed to the calculation speed of the algorithm, since the measurement data need to be available completely.

To carry out the system, first the matrix A is calculated. For this purpose, a radius $R = 0,015$ m and a number of sensors $N = 8$ is assumed. Then equation (3) is used to calculate the time-of-flight data that represent the measured values. The number of iterations is set to $k = 100$. From the resulting set of solutions the one having the least squares with respect to the predetermined values is selected.

Two virtual test problems are generated: (a) radial symmetric ultrasound velocity profile (Figure 9), a random radial symmetric ultrasound velocity profile, with a temperature gradient of 5°C towards the centre of the measurement region (Figure 10). In addition, the temperature randomly varies between the upper and the lower limit of each circle. The numeration of the area elements is illustrated in Figure 3.

In both cases, the ultrasound velocities can be reconstructed very accurately. The standard deviation is 1 m/s (case a) and 8 m/s (case b). From this follows that the used models for ultrasound tomography depict a reliable method to accurately determine the temperature distribution during injection moulding. However, the used model underlay restriction in the near of the melt temperature due to non-linear behaviour of the plastics. For a clear correlation of ultrasound velocity with the temperature, time-of-flight measurements should be performed under defined laboratory conditions. For this, a measurement device is required that allows measurements without any cooling effects. Furthermore, for calculating the temperature additional information of the material, e.g. pVT-relations, must be known in detail, since process parameters like cooling rate influence this behaviour [19]. In addition, the models, especially the designed system matrix and thus the propagation behaviour of the ultrasound wave, underlay no disturbing effects in the virtual test problems. In view of the real process conditions, one must expect that such effects will appear in time-of-flight measurements, such as refractions, scattering and reflection. In this case the system matrix can be extended by beam propagation methods (BPM) or ray-tracing that can be handled with the SART-Algorithm [20].

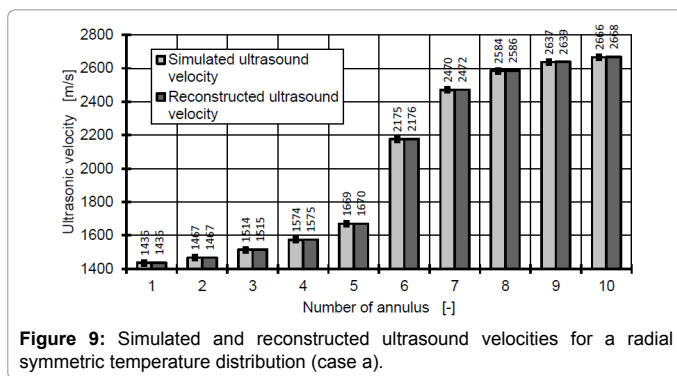


Figure 9: Simulated and reconstructed ultrasound velocities for a radial symmetric temperature distribution (case a).

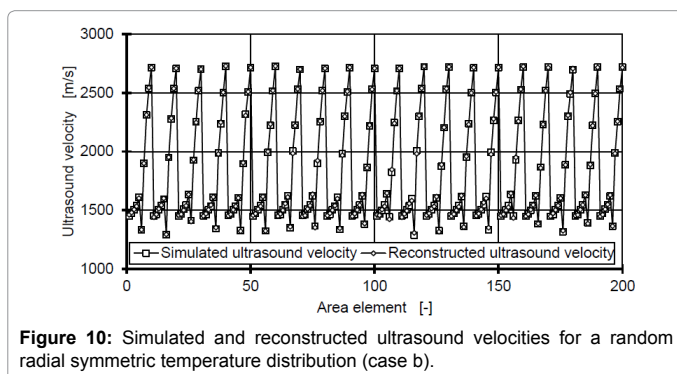


Figure 10: Simulated and reconstructed ultrasound velocities for a random radial symmetric temperature distribution (case b).

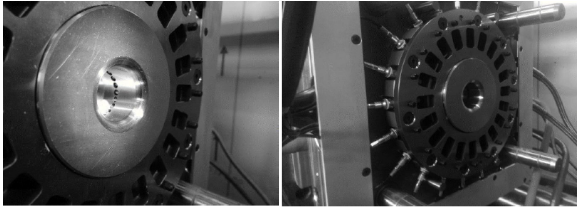


Figure 11: Image of mould shows the measurement region inside the cavity (left) and the radially arranged ultrasound transducer (right).

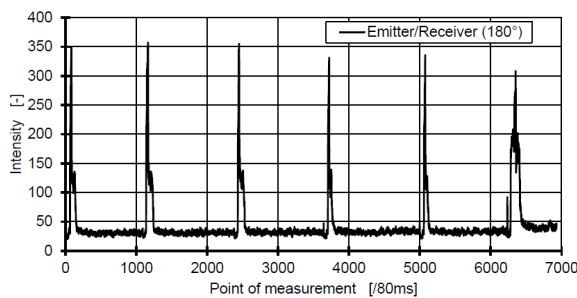


Figure 12: Amplitude-scan during six injection moulding cycles of a receiver opposite to an emitter.

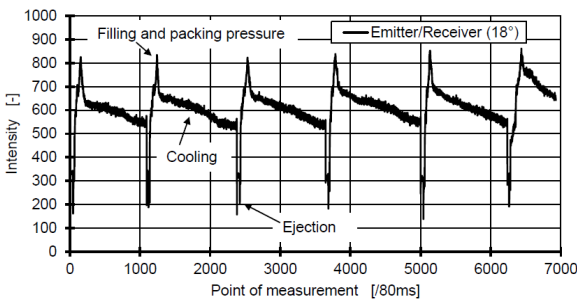


Figure 13: Amplitude-scan during six injection moulding cycles of a receiver next to a receiver.

Pilot experiments

For the non-invasive measurement of the temperature distribution a mould was built containing with 20 ultrasound transducers radially arranged around a cylindrical shaped cavity ($r = 15 \text{ mm}$, $h = 25 \text{ mm}$). Buffer rods shield the ultrasound transducers from the high temperature and their lens-shaped tip scatter the signal within the melt. To provide a tomographic measurement the buffer rods are pushed minimally into the melt by a mechanical mechanism during the measurement and are pulled back before the moulded part is ejected. To avoid circulations of the ultrasound wave within the mould the buffer rods are coated with PEEK. To provide a homogenous pressure within the cross section the mould was designed as compression mould so that a plane pressure can be performed on the moulded part (Figure 11).

To measure the temperature distribution during the injection moulding process a fast detection of the signals is required, since high cooling rates lead to a fast solidification of the moulded part. Furthermore, shrinkage during the solidification leads to separating of the moulded part from the buffer rods and prevent injection of the ultrasound signal into the melt. For this reason, a customised measurement device was designed in cooperation with MACEAS GmbH, Bexbach/Germany that provides a parallelised control per

three transducers. Therewith, a complete measuring cycle (20×19 measurements) can be realised within 80 ms with an accuracy of 10 ns and a standard deviation of 3 ns. The deployed ultrasound transducers are FABP-MSWQC-ALP 2.25×25 (GE Sensing and Inspecting Technologies GmbH, Hürth/Germany) that are excited with a frequency of 2 MHz. For a suitable transmission of the ultrasound signal from the transducer into the buffer rod, petrolatum is used as coupling medium.

First experiments are carried out with the injection moulding machine KraussMaffei 160-1000 CX (KraussMaffei Technologies GmbH, Munich/Germany). Because of the temperature sensitivity of the ultrasound transducer of around 60°C the mould temperature was set up to 50°C , which is adverse for the measurement. The high difference between melt temperature (220°C) and mould temperature leads to a fast solidification and thus shrinkage and warpage. During the process the amplitudes at each receiver were detected. Figures 12 and 13 show the resulting amplitudes of six injection-moulding cycles for an opposite receiver and a next-neighbour receiver, respectively. The signal heavily increases after the filling process and during the packing pressure phase. Especially in Figure 13, the decrease of the signal intensity during the cooling phase can be seen. Since the shrinkage of the moulded part between two neighbouring transducers is affected by the sticking out buffer rods, the connectivity between the moulded part and the transducers is guaranteed. This information is lost in the measurement shown in Figure 12 due to shrinkage of the moulded part, so that no signal can be detected. In Figure 13 the ejection of the moulded part can be seen, as the amplitude drops to around 200. The relative high noise from neighbouring receiver can be explained by ultrasound waves that traverse through the mould. The measurements are highly reproducible with every transducer combination over different injection moulding cycles. In general, this shows the feasibility of ultrasound measurements during the injection moulding process. Even next-neighbour transducer are able to detect noticeable signals, which is beneficial with respect to the spatial resolution, since the number of signals that are detectable produce the maximum spatial resolution of around 3.5 mm^2 with respect to a diameter of the cavity of 30 mm. Due to internal signal processing of the measurement device, it is not yet possible to calculate arrival times of the ultrasound signal. An explanation for this is the complex path of buffer rod, solidifying melt and again buffer rod. This causes a broadening of the ultrasound pulse that is not detectable by the internal software, since calibration of the software was not performed on solidified and molten PP and a much higher signal to noise ratio was expected. New calibration is on-going with the data from the pilot experiment. In future, also signal averaging will be possible to reduce noise.

Conclusion and Outlook

In this work, we present the principle and feasibility of the ultrasound tomography for the spatially resolved temperature measurements of a moulded part during the injection moulding process. Measuring the arrival times of an ultrasound wave emitted by a transducer from different direction allow to reconstruct the distribution of ultrasound velocity in a cross section of a cavity. From this distribution, the temperature field can be calculated using additional material characteristic properties, which can be either determined through simulation or through experiments. Based on the concept of ultrasound tomography, an injection mould was designed, that allows time-of-flight measurements with 20 ultrasound transducers radially arranged around a cylindrical shaped cavity. Lens-shaped buffer rods enable the possibility the scatter the ultrasound wave within the melt, to provide

the necessary information density that is required for the temperature calculation. Furthermore, the buffer rods shield the temperature-sensitive ultrasound transducer from the high temperatures of the melt. In this work, we show that the maximum possible resolution of 3.5 mm² with respect to the described measurement area could be reached, since it was possible to detect noticeable signals at each sensor position. A highly parallelised measurement device allows the acquisition of 380 arrival times within 80 ms. For this reason, several complete datasets can be recorded before, due to shrinkage of the moulded part, no more signals can be detected. Internal signal processing of the measurement device actually prevents to calculate arrival times of the ultrasound signal but amplitude-scans show the general feasibility of ultrasound tomography during injection moulding.

The used model to calculate the temperature from the ultrasound velocity requires several additional material specific data, which should be determined over a wide temperature and pressure range. It could be shown that, using standard tests and models, the used model leads to high inaccuracies, especially in the area of the melt temperature, because of the non-linear behaviour of the material. Due to the high accuracy of the ultrasound measurement device the highest error for the determination of the temperature is thus produced by the used model. Therefore, it is suitable to correlate the ultrasound velocity with the temperature directly under defined temperature and pressure states. This requires the construction of a special measurement device, which prevents cooling of the material. These data would also be less sensitive to the high cooling rates that occur during injection moulding.

Acknowledgements

All presented investigations were conducted in the context of the Collaborative Research Centre SFB1120 "Precision Melt Engineering" at RWTH Aachen University and funded by the German Research Foundation (DFG). For the sponsorship and the support, we wish to express our sincere gratitude.

References

- Ospald F (2014) Numerical simulation of injection molding using Open FOAM. *Proceedings in applied Mathematics and Mechanics* 14: 673-674.
- Shelesh-Nezhad K, Siores E (1997) An intelligent system for plastic injection molding process design. *J of Materials Processing Technology* 63: 458-462
- Zhou H, Li D (2005) Integrated simulation of the injection molding process with stereolithography molds. *Int. J Adv Manuf Technol* 28: 53-60.
- Bendada K, Cole K, Lamontagne M, Simard Y (2003) A hollow waveguide infrared thermometer for polymer temperature measurement during injection moulding. *J Opt A Pure Applied Opt* 5: 464-470.
- Bur AJ, Roth SC, Spalding MA, Baugh DW, Koppi KA, et al. (2004) Temperature gradients in the channels of a single-screw extruder. *Polym Eng Sci* 44: 2148-2157.
- Migler KB, Bur AJ (1998) Fluorescence based measurement of temperature profiles during polymer Processing. *Polym. Eng Sci* 38: 213-221.
- Tzu-Fang C, Ky TN, Szu-Sheng LW, Cheng-Kuei J (1999) Temperature measurement of polymer extrusion by ultrasonic techniques. *Meas Sci Technol* 10: 139.
- Praher B, Straka K, Steinbichler G (2013) An ultrasound-based system for temperature distribution measurements in injection moulding: system design, simulations and off-line test measurements in water. *Meas Sci Technol* 24: 84004.
- Halmen N, Kugler C, Hochrein T, Heidemeyer P, Bastian M (2017) Ultrasound tomography for inline monitoring of plastic melts. *J Sensors Sens Syst* 6: 9-18.
- Yang Y, Yang W, Zhong H (2008) Temperature distribution measurement and control of extrusion process by tomography. *IEEE International Workshop on Imaging Systems and Techniques*.
- Buzug T (2008) *Computed tomography*. Springer-Verlag, Heidelberg, Berlin.
- Kak AC, Slaney M (2001) *Principles of computerized tomographic imaging*. Society for Industrial and Applied Mathematics, Philadelphia.
- Hansen PC, Saxild-Hansen M (2012) AIR tools - A MATLAB package of algebraic iterative reconstruction methods. *J Comput Appl Math* 236: 2167-2178.
- Oakley BA, Barber G, Worden T, Hanna D (2003) Ultrasonic parameters as a function of absolute hydro-static pressure. I. A Review of the Data for Organic Liquids. *J. Phys. Chem. Ref. Data*, 32: 1501-1533.
- Drummer D, Ehrenstein GW, Hopmann C, Vetter K, Meister S, et al. (2012) Analysis and comparative assessment of different process technologies for manufacturing polymer micro-elements. *Mater Sci Eng B* 2: 347-362.
- Hopmann C, Poppe E, Spekowius M, Wipperfurth J, Spina R, et al. (2016) *Integrative Kunststofftechnik 2016*. Shaker Verlag, Aachen.
- Hendee WR, Ritenour ER (2002) *Medical imaging physics*. (4th edn), Wiley-Liss Inc., New York.
- Krautkrämer J, Krautkrämer H (1961) *Werkstoffprüfung mit Ultraschall*. Springer-Verlag OHG, Berlin, Göttingen, Heidelberg.
- Zuidema H, Peters GWM, Meijer HEH (2001) Influence of cooling rate on pVT-date of semi-crystalline polymers. *J Appl Polym Sci* 82: 1170-1186.
- Andersen AH, Kak AC (1984) Simultaneous algebraic reconstruction technique (SART): A superior implementation of the art algorithm. *Ultrason. Imaging* 6: 81-94.